PHILOSOPHICAL TRANSACTIONS OF THE ROYAL SOCIETY A MATHEMATICAL, PHYSICAL & ENGINEERING SCIENCES

A Study of the Oxidation Mechanisms of Some Austenitic Stainless Steels in Carbon Dioxide at 1123K by means of Charged-Particle Nuclear Techniques. II

P. Skeldon, J. M. Calvert and D. G. Lees

Phil. Trans. R. Soc. Lond. A 1980 **296**, 557-565
doi: 10.1098/rsta.1980.0193

A STUDY OF THE OXIDATION MECHANISMS OF SOME AUSTENITIC STAINLESS STEELS IN CARBON DIOXIDE AT 1123K BY MEANS OF CHARGED-PARTICLE NUCLEAR TECHNIQUES. II

BY P. SKELDON†, J. M. CALVERT‡ AND D. G. LEES†

† *Metallurgy Department, Manchester University, Manchester, M13 9PL, U.K.*

‡ *Physics Department, Manchester University, Manchester, M13 9PL, U.K.*

(*Communicated by R. B. Nicholson, F.R.S. – Received 10 January 1979*)

[Plate 1]

CONTENTS

The oxidation behaviour in carbon dioxide at 1123 K and a pressure of approximately 0.1 MPa of a sample of 20% (by mass) Cr, 25% (by mass) Ni, Nb-stabilized steel (the standard steel) coated with ceria has been investigated by means of charged-particle nuclear techniques and conventional methods. The nuclear techniques were used to study the growth mechanism, thickness and surface composition of the oxide.

The scale consisted of an outer spinel layer and an inner layer of Cr_2O_3. It is not known if there was a silicon-rich layer at the oxide–metal interface because the oxide was adherent. The growth-mechanism of the oxide was studied with ^{18}O as a tracer and was found to grow primarily by oxygen diffusion, although there was indirect evidence for some cation diffusion. The growth-mechanism of the oxide is quite different from that on the standard steel without the ceria, and it is suggested that this is because ceria segregates to dislocations and grain-boundaries in the oxide. In the light of the results for the standard steel it is not clear if cerium reduces the cation diffusion *and* increases the oxygen diffusion, or merely reduces the cation diffusion.

1. Introduction

In associated investigations (Skeldon *et al.* 1980*a*, *b*, subsequently referred to as I and III), charged-particle nuclear techniques were used to study the oxide growth mechanisms when a niobium-stabilized austenitic steel (the standard steel) and a similar steel strengthened with a dispersion of titanium nitride were heated in carbon dioxide at 1123 K and a pressure of approximately 0.1 MPa. It is known that the oxide-adhesion of the standard steel is improved and the oxidation rate reduced if ceria is deposited on the surface of this steel before oxidation under these conditions (Tyzack *et al.* 1974). The present paper reports the results of an investigation of the oxidation mechanism of a sample of the cerium-treated standard steel with the use of the nuclear techniques referred to above.

2. Previous work

The effects of cerium on the oxidation of this alloy in the temperature range 1023–1173 K have been investigated by means of a treatment which leaves a deposit of CeO_2 on the alloy surface (Tyzack *et al.* 1974). The unoxidized alloy was dipped in an alcoholic solution of ceric ammonium nitrate of concentration 50 g/l, dried and heated at 623–673 K for a few minutes, a process that typically left about 50 μg cm^{-2} of CeO_2 on the alloy surface. Tests lasting 5000 h with intermittent cooling for weighing of the samples showed that the ceria treatment reduced the gross mass gain and the total mass percentage spalled by, on average, factors of two and four respectively. The scales on the ceria treated samples consisted of Cr_2O_3 and probably $MnCr_2O_4$, the latter being present at the outside of the scale. Iron and nickel were not detected. The CeO_2 was found mainly at the scale surface but cerium was also present in the scale and at the alloy–oxide interface. A gold stripe placed on the alloy surface remained visible when the specimen was oxidized, which indicates that the oxide grew mainly by oxygen diffusion, but after prolonged oxidation the stripe became slightly less obvious.

3. Experimental procedure

(*a*) *Sample preparation*

The specimen of cerium-treated standard alloy was provided by Risley Nuclear Power Development Establishment; its composition is given in table 1. The specimen size was approximately 2 cm × 2 cm × 0.05 cm. It was abraded with 180 silicon carbide, sealed in an evacuated silica tube, annealed for 30 mins at 1323 K and then the cerium oxide deposit produced on the surface in the manner described earlier in this paper.

(*b*) *Sample oxidation*

Oxidation times are given in table 2.

The specimen was oxidized at 1123 K in dried, flowing CO_2 at 0.1 MPa pressure at Risley. It was then cooled to room temperature and oxidized at Manchester in static carbon dioxide enriched in $C^{18}O_2$ as described in detail in I. The mass gain after oxidation at Risley, including spalled oxide, was 0.056 mg/cm², which corresponds to an oxide thickness of approximately 0.35 μm. (Note that the result from elastic scattering measurements does not agree with this figure, § 4*a*.) The mass-gain excluding the spalled oxide was 0.053 mg/cm². Unlike the samples used in I and III, this was the only specimen that was cooled to room temperature between oxidations. It is occasionally convenient to refer to natural carbon dioxide as $C^{16}O_2$ and the isotopically enriched gas as $C^{18}O_2$. The handling of the $C^{18}O_2$ is described fully in I.

TABLE 1. ALLOY COMPOSITION (% BY MASS)

Fe	Cr	Ni	Mn	Si	Nb	C
bal.	20.3	25.1	0.6	0.64	0.64	0.03

TABLE 2. OXIDATION TIMES (HOURS)

total	natural CO_2	$C^{18}O_2$
618	500	118

(*c*) *Charged-particle nuclear techniques*

The nuclear technique used in this investigation to determine the ^{18}O concentration profile has been discussed elsewhere (Calvert *et al.* 1974) and also briefly in I. The $^{18}O(p,\alpha)^{15}N$ reaction was used to determine the concentration of ^{18}O in the scale as a function of depth; elastic scattering was used as in I for normalization, and for determining the scale thicknesses and the composition of the oxide at the oxide–gas interface. The principles underlying the use of elastic scattering measurements in this work are discussed briefly in I.

4. RESULTS

(*a*) *Oxide thickness*

The oxide thickness calculated from elastic scattering measurements was *ca.*1 μm after oxidation in $C^{16}O_2$ and *ca.* 1.6 μm after oxidation in $C^{18}O_2$. The former value is different from that obtained from mass-gain measurements, § 3*b*. We prefer the value from elastic scattering because there is always a possibility of the mass-gain measurements being invalidated by failure to collect all the spalled scale.

(*b*) *Appearance of the oxidized sample*

The specimen had a grey, adherent scale.

(*c*) *Composition of the scale*

X-ray diffraction measurements showed the presence of Cr_2O_3, spinel and CeO_2 in the scale (table 3). The spinel produced the strongest diffraction peaks, and careful measurements gave a

lattice parameter of 0.8425 nm, which is consistent with $MnCr_2O_4$ or $MnFe_2O_4$. Energy-dispersive X-ray analysis (table 4) indicated that the scale was chromium-rich and contained significant amounts of manganese and iron. A small amount of nickel was detected. (As the scale was on the alloy, these results could have been affected by signals coming from the substrate.) X-ray diffraction measurements before and after the $C^{18}O_2$ oxidation showed that the amount of CeO_2 had decreased by a factor of approximately two. Elastic scattering experiments identified chromium, manganese, iron and cerium in the surface of the scale (figure 1).

TABLE 3. X-RAY DIFFRACTION RESULTS

oxide	Cr_2O_3	spinel	CeO_2
	medium	strong	strong

TABLE 4. ENERGY DISPERSIVE X-RAY ANALYSIS RESULTS

Si	Ti	Cr	Mn	Fe	Ni	Ce
1.0	n.d.	59.6	19.3	15.4	2.4	2.3

n.d. denotes not detected.

The maximum cerium concentration was located at the surface of the scale and the results suggested that the concentration decreased with depth in the manner of a diffusion-type profile, but the possibility that the initial deposit of CeO_2 was non-uniform and hence gave rise to this profile cannot be ruled out. These results also show that the cerium concentration at the scale surface after oxidation in $C^{18}O_2$ had decreased by a factor of two compared with the value before, but in this case (in contrast to the X-ray measurements), we cannot eliminate the possibility that different areas of the specimen were examined in the two elastic scattering experiments and that the cerium content was different in the two areas.

From these results the scale is believed to be composed of an inner layer of Cr_2O_3 and an outer layer which contains manganese, iron and chromium. Energy-dispersive X-ray measurements could not be used (as in III), to determine if there was a silicon-rich layer at the oxide–metal interface, because the scale did not spall.

(*d*) *Scale morphology* (figures 2*a*, *b*, plate 1)

The main features shown by these pictures may be summarized as follows:

(i) the scale was not buckled, was fully adherent, and had a nodular appearance;

(ii) scratch marks from grinding were clearly visible on the top of the scale;

(iii) whiskers were present at the oxide surface;

(iv) the surface of the scale (which the considerations presented in §4*c* suggest was spinel) had a fine-grained appearance.

(*e*) *Measurement of oxide crystallite size*

An attempt was made to determine the size of the crystallites in the scale using the broadening of X-ray diffraction peaks. The technique has been described by Peiser *et al.* (1955). A test of the method, with Al_2O_3 powder which was stated by the manufacturers to have a particle size of 0.05 μm, gave a value of 0.03 μm which is considered to be in satisfactory agreement with

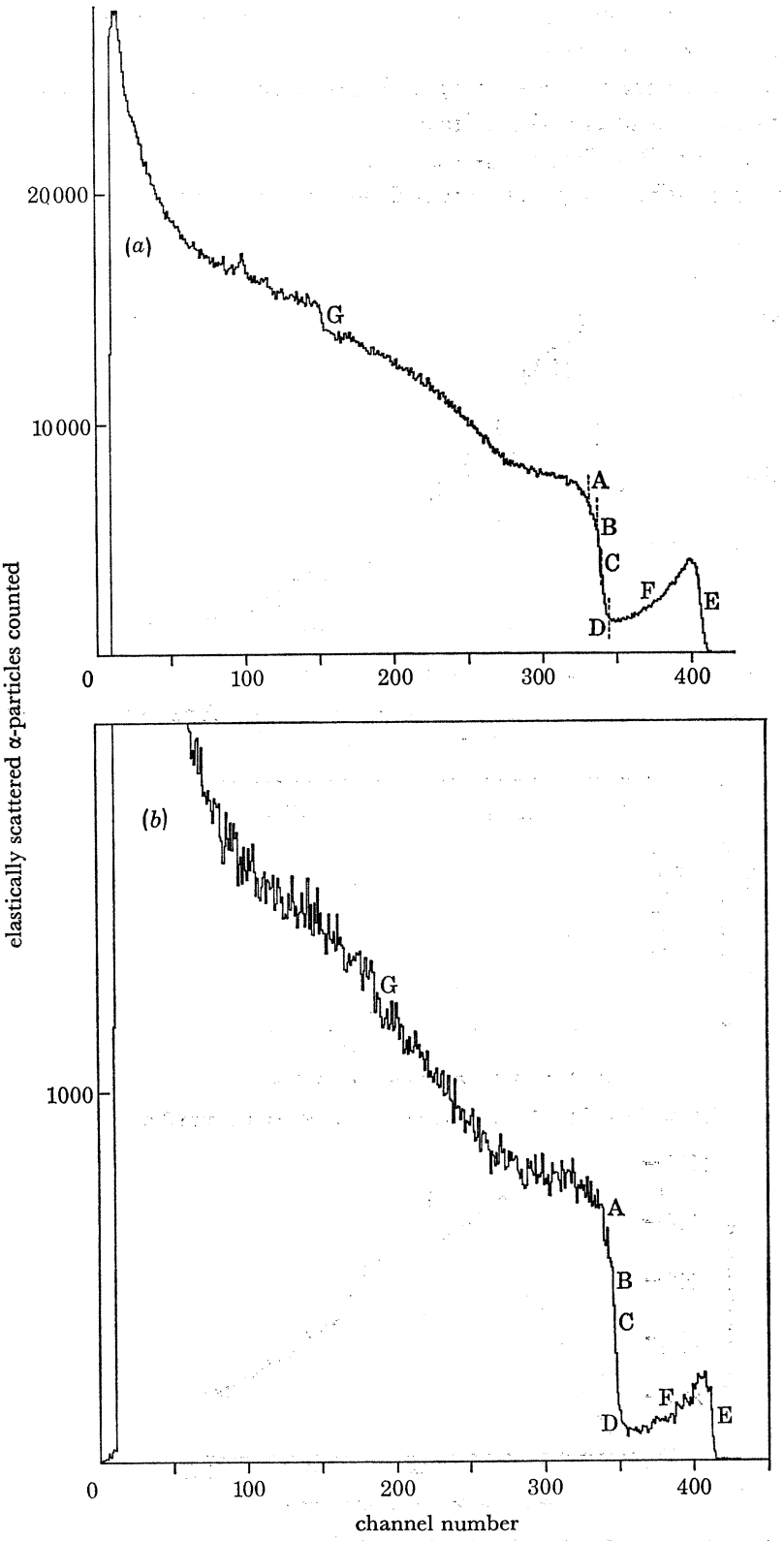

FIGURES 1*a*, *b*. Particle-yield plotted against channel number for α-particles elastically scattered from the oxidized sample, side A. Increasing channel number corresponds to increasing particle energy. The incident α-particle energy was 4 MeV. (i) Particles scattered at the surface of the oxide: A, from chromium; B, from manganese; C, from iron; D, from nickel; E, from cerium; G, from oxygen. (ii) Particles scattered beneath the surface of the oxide: F, from cerium. 1 (*a*) The sample after oxidation in $C^{16}O_2$ and before oxidation in $C^{18}O_2$. 1 (*b*) The sample after oxidation in $C^{18}O_2$.

the quoted figure. However, when the technique was applied to the scale on the steel sample, a number of problems were encountered:

(i) the diffraction peaks were not very strong and contained considerable noise, which made accurate measurements of the peak-width difficult;

(ii) certain spinel and Cr_2O_3 diffraction peaks overlapped;

(iii) only two or three diffraction peaks were sufficiently clear to be of any use.

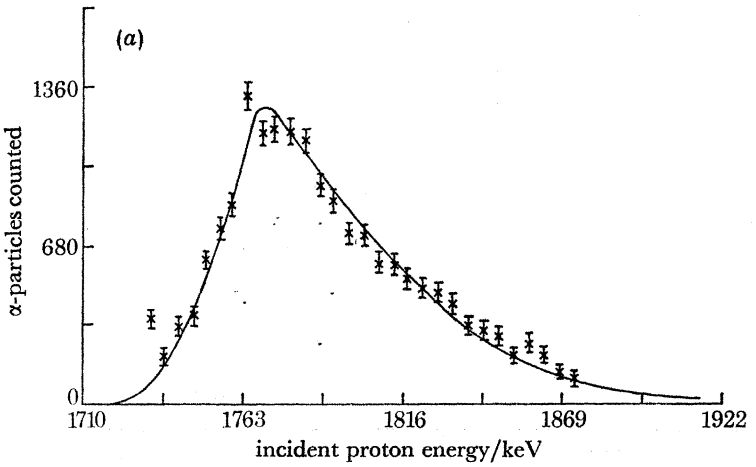

FIGURE 3 (*a*) α-Particle yield plotted against incident proton energy for side A. A value of 1.1×10^{-14} cm^2 s^{-1} was used in the complementary error function.

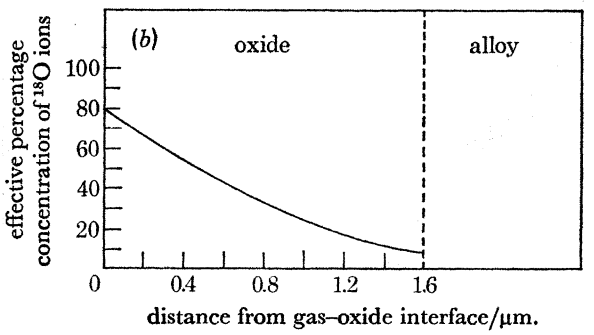

FIGURE 3 (*b*) The ^{18}O distribution deduced from figure 3*a*.

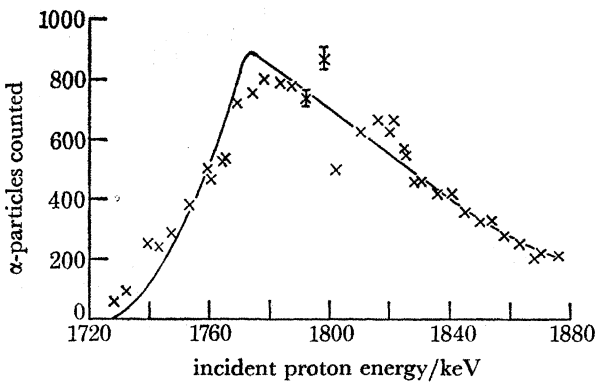

FIGURE 4. α-Particle yield plotted against incident proton energy for side B. A value of 2.5×10^{-14} cm^2 s^{-1} was used in the complementary error function. The effective concentration of ^{18}O at the oxide–gas interface was the same as that for side A.

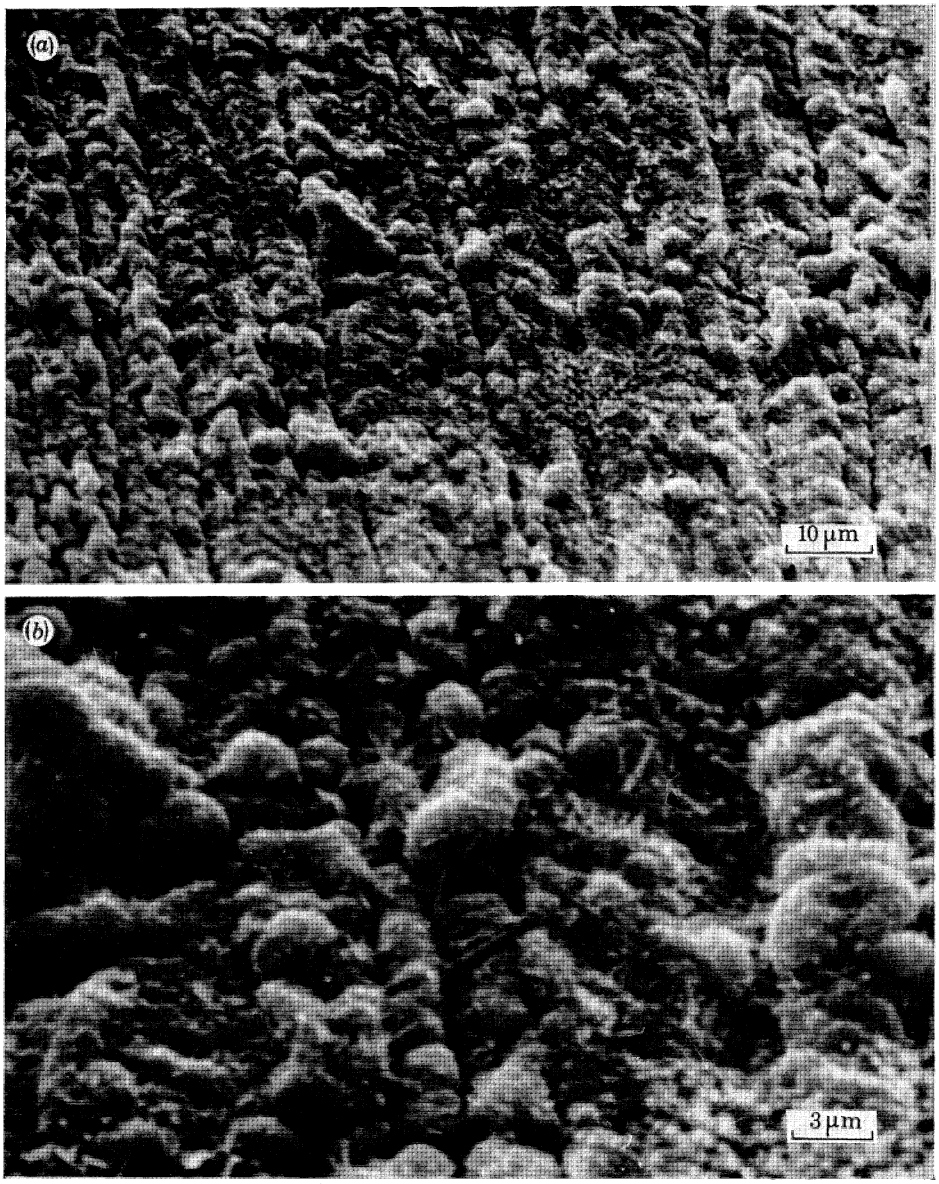

FIGURE 2 (*a*, *b*). The surface of the scale. Electron acceleration energy = 30 keV.

(*Facing p.* 562)

PHILOSOPHICAL TRANSACTIONS OF THE ROYAL SOCIETY A MATHEMATICAL, PHYSICAL & ENGINEERING SCIENCES

The few points that could be plotted and the errors associated with each point prevented an accurate measurement of the crystallite size. However, the measurements indicate that the Cr_2O_3 layer has a crystallite size of approximately 0.1 μm.

(*f*) *The* ^{18}O *tracer distributions*

The results are shown in figures 3*a*, *b* and 4. The ^{18}O distributions are similar to the group 1 distributions for the TiN dispersion-strengthened steel discussed more fully in III. Briefly, the distribution has the following characteristics:

(i) it falls monotonically from the scale surface and has the form of a complementary error function;

(ii) the concentration of ^{18}O at the scale surface is less than 100%; the corrections required when calculating this value are discussed in detail in §3*e* of I, and tended to over-estimate the concentration of ^{18}O in the surface of the scale.

5. Discussion

(*a*) *Oxide growth-mechanism*

The cerium-treated steel formed a very similar scale to the standard steel (I) and the TiN dispersion-strengthened steel (III). The evidence suggests that in each case the scales consisted of an outer spinel layer, inside which was a layer of Cr_2O_3 and, in the case of the standard steel and the dispersion-strengthened steel, a silicon-rich layer at the oxide–metal interface. As discussed earlier, we do not know if there was a silicon-rich layer on the cerium-treated steel. Despite these similarities, there were marked differences in the growth mechanisms. In the case of the cerium-treated steel, the ^{18}O tracer results show that the contribution of oxygen diffusion to growth of the scale was substantial. The interpretation of graphs of α-yield plotted against incident proton energy, which suggest that oxygen diffusion has occurred, is discussed in detail in the appendix to III. In the present case we have evidence which is not available for the specimens of the TiN dispersion-strengthened alloy, namely the spectrum of elastically scattered α-particles obtained at the end of the $C^{16}O_2$ oxidation and before the $C^{18}O_2$ oxidation (figure 1*a*). The slope of the part of this graph that corresponds to the oxide–metal interface indicates that the fraction of the surface area that is very thin is very small. Therefore, the model proposed in figure 14*b* of III does not apply, and the shape of the α-yield against incident proton energy graphs cannot be caused by surface roughness. Evidence that the oxide grew primarily by oxygen transport is provided by the cerium distributions shown by figures 1*a* and 1*b*, because the ceria has acted as a marker and been carried outwards by the growing oxide. The oxide growth mechanism proposed here agrees with the observation of Tyzack *et al.* (1974) that a gold stripe remained clearly visible after oxidation, although it is interesting to note that it became slightly less obvious after long testing. The presence of whiskers at the oxide–gas interface suggests that some cation diffusion also occurred. As we have stated above, we believe that a spinel layer was present on the outside of the Cr_2O_3 layer. Either this layer was so thin that it had no effect on our results (for the reasons given in §3*e* of I), or it, too, grew primarily by oxygen transport. The absence of scale-buckling on this sample may indicate that new oxide was not formed within the original layer, or it could be that it did do so but was only formed at grain boundaries parallel to the oxide–metal interface (this question has already been discussed in §5 of I for the case of the standard steel) or that such stresses were produced but that, nevertheless, the oxide–metal adhesion was sufficient to prevent oxide buckling.

PHILOSOPHICAL TRANSACTIONS OF THE ROYAL SOCIETY A MATHEMATICAL, PHYSICAL & ENGINEERING SCIENCES

(b) The effect of oxygen-active elements on the oxide growth-mechanism

Cerium belongs to a group of elements that are known to have a beneficial effect on oxide–metal adhesion, which have in common a high affinity for oxygen and which are thus known in this context as oxygen-active elements. In the case of Cr_2O_3 scales formed on nickel-based alloys, elements from this group have been shown to change the growth mechanism from one in which cation diffusion was predominant to one in which oxygen diffusion was predominant (Giggins & Pettit 1971; Wallwork & Hed 1971; Stringer *et al.* 1972). The ^{18}O tracer results of the present study confirm this, and the results reported in III show that, in the scale on the TiN dispersion-strengthened alloy, oxygen diffusion is substantial, a fact that we attribute to the presence of titanium in the scale. Stringer *et al.* (1972) have suggested that the oxygen-active elements change the growth mechanism in this way because they keep the oxide grain size smaller and that this (*a*) promotes oxygen diffusion because oxygen possibly diffuses along oxide grain boundaries faster than does chromium and (*b*) probably retards or eliminates the short-circuit diffusion of chromium by reducing the dislocation density. However, evidence that has been published since this theory was proposed does not seem to support it. Stringer *et al.* showed that the oxide on the dispersion-containing parts of an Ni-20% (by mass) Cr-3% (by volume) Y_2O_3 alloy had a grain size of *ca.* 0.1 μm. Wright *et al.* (1975) quote values of 0.3–0.5 μm for the grain size of the oxide formed on the same alloy, and Wright & Wilcox (1974) values in the range 0.5–1.0 μm for the oxide formed on an Fe-16% (by mass) Cr-3% (by volume) Y_2O_3 alloy. Stringer *et al.* found that the oxide that grew on dispersion-free areas of their alloy had a grain size of 0.2–0.5 μm. Thus, although this grain size is much larger than that of the oxide that grew over the dispersion-containing areas of the same specimen studied by Stringer *et al.*, this is not the case when we compare it with the results of the other workers. If, as seems reasonable, we assume that all the oxide that grew on the dispersion-containing material did so primarily by oxygen diffusion and that the oxide on the dispersion-free material grew primarily by cation diffusion, then the results do not support the theory. It must be emphasized that the evidence is sparse and indirect at present, but we believe that there is a need for an alternative theory for the effect of oxygen-active elements on the scale growth mechanism.

We suggest that the oxygen-active elements may alter the oxide growth mechanism by segregating to oxide grain-boundaries and dislocations, and simultaneously hindering cation diffusion and possibly promoting oxygen diffusion along these. Nanni *et al.* (1976) have shown that yttrium segregates, presumably as yttria, to grain boundaries in Al_2O_3. It is suggested that this is linked with the fact that the ionic radius of yttrium is much greater than that of aluminium. The ionic radii of the oxygen-active elements are also greater than that of chromium, and therefore it seems reasonable to suppose that they segregate to grain-boundaries in Cr_2O_3. The exception to this is the Ti^{4+} ion, which has a radius almost identical to that of the Cr^{3+} ion. If our theory is correct, we must assume that titanium is present in the divalent state (when the ionic radius is much larger) or that there is some other reason for it segregating to the grain-boundaries in Cr_2O_3.

As we have pointed out, indirect evidence suggests that some cation diffusion occurred in the oxide scale on the cerium-treated alloy, and this is also the case for the TiN dispersion-strengthened alloy (III). It is interesting to note that scales on the latter alloy sometimes buckled, while that on the cerium-treated specimen did not. This may indicate that titanium

is less efficient in blocking cation diffusion than is cerium, but this is not necessarily so; for example, it could be that cerium improves the oxide–metal adhesion better than does titanium.

In the light of the observation that some oxygen diffusion occurs in the scale on the standard alloy (I), it is interesting to speculate whether the oxygen-active elements change the relative amounts of cation and oxygen diffusion in Cr_2O_3 by decreasing the cation diffusion *and* promoting oxygen diffusion, or merely by decreasing the cation diffusion. As the cerium treatment reduces the oxidation rate of this alloy (Tyzack *et al.* 1974) and as oxygen-active elements have been shown to have this effect on the oxidation rate of other alloys, the latter explanation seems quite likely.

6. Conclusions

^{18}O tracer measurements (I) have shown that the oxide-scale which formed on a 20% (by mass) Cr, 25% (by mass) Ni, Nb-stabilized steel in CO_2 at 1123 K grew primarily by cation diffusion, but that some oxygen diffusion also occurred. When this alloy was coated with ceria the oxide growth-mechanism changed markedly, so that the scales grew primarily by solid-state oxygen diffusion, although indirect evidence indicates that some cation diffusion also occurred. It is suggested that the cerium changes the oxide growth mechanism by segregating to grain boundaries and dislocations in the oxide. It is not clear if the cerium decreases cation diffusion *and* promotes oxygen diffusion, or merely decreases the cation diffusion.

The scale on the cerium-treated alloy is believed to consist of an outer layer of spinel and an inner layer of Cr_2O_3. It is not known if a silicon-rich layer was present at the oxide–metal interface.

This work is being continued; in particular, specimens with smoother surfaces are being investigated.

We are grateful to the Science Research Council for financial support for one of us (P.S.) and for a research grant which assisted the work, and to Risley Nuclear Power Development Establishment for the provision of the cerium-treated specimen. We are also grateful to Mr Stuart MacLachlan for assistance with the determination of the ^{18}O distributions.

References

Calvert, J. M., Derry, D. J. & Lees, D. G. 1974 *J. Phys. D.* **7**, 940–953.
Giggins, C. S. & Pettit, F. S. 1971 *Metall. Trans.* **2**, 1071–1078.
Nanni, P., Stoddart, C. T. H. & Hondros, E. D. 1976 *J. Mater. Chem.* **1**, 297–320.
Peiser, H. S., Rooksby, H. P. & Wilson, A. J. C. 1955 *X-ray diffraction by polycrystalline materials*. London: The Institute of Physics.
Skeldon, P., Calvert, J. M. & Lees, D. G. 1980*a* *Phil. Trans. R. Soc. Lond.* A **296**, 545–555.
Skeldon, P., Calvert, J. M. & Lees, D. G. 1980*b* *Phil. Trans. R. Soc. Lond.* A **296**, 567–580.
Stringer, J., Wilcox, B. A. & Jaffee, R. I. 1972 *Oxidat. Metals* **5**, 11–47.
Tyzak, C., Cowen, H. C., Farrow, M., Longton, P. B. & Whitlow, W. H. 1974 In *Corrosion of steels in* CO_2 (ed. D. R. Holmes, R. B. Hill & L. M. Wyatt), pp. 359–368. British Nuclear Energy Society.
Wallwork, G. R. & Hed, A. Z. 1971 *Oxidat. Metals* **3**, 229–241.
Wright, I. G. & Wilcox, B. A. 1974 *Oxidat. Metals* **8**, 283–301.
Wright, I. G., Wilcox, B. A. & Jaffee, R. I. 1975 *Oxidat. Metals* **9**, 275–305.

PHILOSOPHICAL TRANSACTIONS OF THE ROYAL SOCIETY A MATHEMATICAL, PHYSICAL & ENGINEERING SCIENCES

PHILOSOPHICAL TRANSACTIONS OF THE ROYAL SOCIETY A MATHEMATICAL, PHYSICAL & ENGINEERING SCIENCES

FIGURE 2 (*a*, *b*). The surface of the scale. Electron acceleration energy = 30 keV.